In vitro and *In vivo* Targeting Properties of Iodine-123- or Iodine-131–Labeled Monoclonal Antibody 14C5 in a Non–Small Cell Lung Cancer and Colon Carcinoma Model

Ingrid Burvenich,[1] Steve Schoonooghe,[2] Bart Cornelissen,[1] Peter Blanckaert,[1] Elisabeth Coene,[3] Claude Cuvelier,[3] Nico Mertens,[2] and Guido Slegers[1]

Abstract

Purpose: The monoclonal antibody (mAb) 14C5 is a murine IgG1 directed against a yet undefined molecule involved in cell substrate adhesion found on the surface of malignant breast cancer tissue. mAb 14C5 is able to inhibit cell substrate adhesion and invasion of breast cancer cells *in vitro*. In normal tissues as well as in the stroma surrounding *in situ* carcinomas of the breast, no expression of the antigen 14C5 occurs. The aim of this study was to investigate the *in vitro* and *in vivo* targeting properties of ^{123}I- and ^{131}I-labeled mAb 14C5 as a novel agent for radioimmunodetection and radioimmunotherapy.

Experimental Design: Internalization of mAb 14C5 was investigated with ^{125}I-labeled mAb 14C5 and by confocal laser scanning microscopy. Biodistribution studies of ^{131}I-labeled mAb 14C5 and planar gamma imaging were done in nude mice bearing an A549 (non–small cell lung carcinoma) or a LoVo (colon carcinoma) tumor.

Results: Internalization studies with both A549 and LoVo cells showed that ^{125}I-labeled mAb 14C5 is slowly internalized with ~30% of the initially bound mAb 14C5 internalized after 2 hours at 37°C. Internalization of mAb 14C5 could be visualized with confocal laser scanning microscopy. *In vivo*, radioisotope uptake peaked at 24 hours for both tumor models ($n = 5$) with no significant difference in percentage of injected dose/g tissue (A549 10.4 ± 0.8 and LoVo 9.3 ± 0.8). Via planar gamma camera imaging, A549 lung tumors as well as LoVo colon tumors could be clearly visualized.

Conclusions: The *in vitro* and *in vivo* targeting properties of ^{123}I- and ^{131}I-labeled mAb 14C5 are promising and could provide a new antibody-based agent for radioimmunodetection and radioimmunotherapy of patients bearing antigen 14C5–expressing tumors.

Radioimmunodetection and radioimmunotherapy involve the use of anticancer antibodies conjugated with diagnostic and therapeutic radionuclides, respectively. Encouraging results have been achieved with this technology in the management of hematopoietic neoplasms (1–5). On the contrary, solid tumors have been less responsive, but several articles report on the potential of radiolabeled antibodies targeting minimal or micrometastatic disease (6–8). Despite these encouraging results, new treatment strategies are required for the cure of patients with advanced breast cancer.

In the industrialized world, breast cancer is second only to lung cancer as the leading cancer causing death in women (9). Many monoclonal antibodies (mAb) have been developed for targeting tumor antigens with high expression on malignant breast cancer cells, including HER-2/*neu* (10, 11), epidermal growth factor receptor, carcinoembryonic antigen, MUC1 (12), Lewis Y (13), and mAb 14C5 (14). The murine mAb 14C5 was obtained by immunizing BALB/c mice with the membrane fraction of SK-BR-3 human breast carcinoma cells (14). mAb 14C5 recognizes an epitope at the extracellular domain of a membrane antigen, which plays a role in cell substrate adhesion. This could be deduced from the inhibition of adhesion of SK-BR-3 and MCF-7 breast cancer cells to culture plastic, pronectin-, osteopontin-, and vitronectin-coated wells (14). The inhibition on fibronectin-coated wells was weaker. In addition, a confrontation experiment with precultured embryonic heart fragments showed that the cell substrate adhesion of breast cancer cells could be inhibited or at least delayed (14, 15).

The antigen 14C5 is present in high amounts on the tumor surface of *in situ* and invasive breast cancer tissue (15). Biopsy specimens from various normal human tissues were investigated for the expression of the antigen 14C5. Normal epithelial, muscle, and connective tissues that did not show staining with mAb 14C5 were skin, thyroid, parathyroid, colon, stomach, lung, uterine tube, ovary, ureter, urethra, lymph node, nerve, chondroid tissue, skeletal muscle, esophagus, and artery (14, 15). Sometimes, low-level staining of myoepithelial

Authors' Affiliations: [1]Laboratory of Radiopharmacy, [2]Department of Biomedical Research, Flanders Institute of Biotechnology (VIB), and [3]N. Goormaghtigh Institute of Pathology, University of Ghent, Ghent, Belgium

Received 12/6/04; revised 7/15/05; accepted 7/26/05.

The costs of publication of this article were defrayed in part by the payment of page charges. This article must therefore be hereby marked *advertisement* in accordance with 18 U.S.C. Section 1734 solely to indicate this fact.

Requests for reprints: Ingrid Burvenich, Laboratory of Radiopharmacy, University of Ghent, B-9000 Ghent, Belgium. Phone: 32-9-2648063; Fax: 32-9-2207424; E-mail: ingrid.burvenich@ugent.be.

doi:10.1158/1078-0432.CCR-04-2503

cells is observed in biopsies of breast tissue and in tubular cells of the kidney. In normal tissues, the stroma is always negative (15). Fibroblasts that surround invasive carcinoma cells express antigen 14C5, whereas the antigen 14C5 is absent in normal fibrous tissue and in fibrous tissue surrounding noninvasive islands of malignant cells (15). In most investigated invasive ductal carcinomas, there was staining not only of the cytoplasmic membrane of the tumor cells but also of cytoplasmic membrane extensions (14). High-level expression of antigen 14C5 on malignant tissue and no or little expression of antigen 14C5 on normal tissues make the antigen 14C5 a potential target for use in radioimmunodetection and radioimmunotherapy.

Immunoprecipitation studies showed two major fragments, with ~50 and 90 kDa as molecular weight (14, 15). The cell substrate inhibition and the immunohistochemical staining on the cell membrane extensions of highly invasive tumor cells suggest a molecule related to the family of integrins. The integrins, a family of related membrane receptors involved in cell-cell and cell-matrix interactions, are heterodimeric complexes of α and β subunits expressed on the cell membrane (16). The molecular weight of antigen 14C5 is similar to the molecular weight of the 85-kDa β-chain of the $\alpha_v\beta_3$ vitronectin receptor (17). However, when the expression of antigen 14C5 is compared with the expression of the different integrin subunits in breast tissue by immunohistochemical methods, none of these subunits seem to overlap with the expression of antigen 14C5 (18–20).

An important future role of mAb 14C5 may lie in the ability of this antibody to prevent the spread of tumor cells into the patient. Moreover, the expression characteristics of the antigen 14C5 are suitable for possible use of the mAb 14C5 in radioimmunodetection and radioimmunotherapy. Depending on the isotope selected, ^{123}I-labeled mAb 14C5 could be used for tumor diagnosis and ^{131}I-labeled mAb 14C5 could be used to kill both primary tumor cells and metastatic cells. mAb 14C5 has already been labeled with ^{123}I in high radiochemical yields and purities while maintaining good *in vitro* and *in vivo* stability and *in vitro* binding properties (21). This study explores the targeting properties *in vivo* of mAb 14C5 bound to ^{123}I and ^{131}I in nude mice bearing an A549 lung or a LoVo colon tumor. Biodistribution and gamma camera imaging studies were done, and internalization was studied with ^{125}I-labeled mAb 14C5 *in vitro*. Because the antigen has not yet been identified, the antigen expression was studied on a variety of tumor cell types by both immunocytochemical staining and flow cytometry to investigate its practical value.

Materials and Methods

Antibodies. The 14C5 antibody-producing hybridoma was derived from the fusion of NSO myeloma cells with spleen cells from BALB/c mice immunized with the human breast carcinoma cell line SK-BR-3 (14). Hybridoma cells produced mAb 14C5 in Integra CL 350 flasks (Elscolab, Kruibeke, Belgium) containing protein-free hybridoma medium (Invitrogen, Merelbeke, Belgium). mAb 14C5 was protein G purified (Amersham Biosciences Europe, Roosendaal, the Netherlands) from concentrated supernatant and dialyzed against PBS (pH 7.4). The purity of the antibody was evaluated by SDS-PAGE using reducing and nonreducing conditions. The 9E10 mAb (anti-c-myc, mouse IgG1, Becton Dickinson, Erembodegem-Aalst, Belgium) was used as a control for a specific Fc receptor binding during flow cytometric analysis. Alexa Fluor 488–conjugated goat anti-mouse IgG antibody (Invitrogen) was used during flow cytometry and confocal laser scanning microscopy. The anti–integrin β_1 mAb (IgG1, Becton Dickinson) was used as a control for nonspecific binding in biodistribution studies.

Cell lines. HT-29, LoVo, Capan-1, Capan-2, and C32 were a kind gift of J&J Pharmaceutical Research & Development (Beerse, Belgium). HT-1080, A2058, A549, AsPC-1, and MDA-MB-231 were obtained from the Laboratory of Tumor and Developmental Biology (University of Liege, Liege, Belgium). OVCAR-3, HeLa, K-562, and BT-20 were obtained from the Department of Molecular Biomedical Research (Flanders Institute of Biotechnology, Ghent, Belgium). SK-BR-3, MCF-7, T-47D, LN-229, Colo16, 791T, and MOLT-4 were obtained from the N. Goormaghtigh Institute of Pathology, University of Ghent (Ghent, Belgium). All cell lines were cultured in standard medium with supplements according to the American Type Culture Collection (Manassas, VA) recommendations, except for Colo16, K-562, and MOLT-4 grown in RPMI 1640 containing 10 mmol/L HEPES and 10% fetal bovine serum (Cambrex, Verviers, Belgium) and 791T grown in DMEM containing 10% fetal bovine serum. All cells were cultured at 37°C in a 5% CO_2 humidified incubator and passaged with 0.05% trypsin-0.02% EDTA.

Immunocytochemical study. Confluent tumor cell lines were harvested by cell scraping and washing twice with PBS. Cells were cytocentrifuged for 5 minutes at 180 × *g* and fixed in acetone for 10 minutes. For immunocytochemical detection, an avidin-biotin system was applied (DakoCytomation, Heverlee, Belgium). mAb 14C5 (1 μg/mL) was incubated for 1 hour in PBS with 5% bovine serum albumin (BSA; Sigma-Aldrich, Bornem, Belgium) at room temperature. The sample was then incubated with biotinylated anti-mouse immunoglobulins for 15 minutes; the avidin-peroxidase complex was added for 15 minutes followed by 3-amino-9-ethylcarbozole (DakoCytomation) for 10 minutes as chromogen. Between each step, cells were washed twice with PBS. Cells were counterstained with Mayer's hematoxylin and mounted in Aquatex mounting medium (VWR International, Leuven, Belgium). Negative control cells were obtained by omitting the primary antibody.

Flow cytometry. Confluent cells were harvested using cell dissociation buffer (Invitrogen). Aliquots of 2×10^5 cells were incubated with mAb 14C5 (10 nmol/L) in PBS-0.5% BSA-0.02% (w/v) sodium azide (Sigma-Aldrich) on ice. After washing the cells with PBS-0.5% BSA-0.02% sodium azide, cells were incubated with Alexa Fluor 488–conjugated goat anti-mouse on ice for 1 hour. Again, cells were washed with PBS-0.5% BSA-0.02% sodium azide and suspended in a final volume of 300 μL PBS-0.5% BSA-0.02% sodium azide. In control samples, the primary antibody was omitted. For isotype control, mAb 9E10 (10 nmol/L) was used instead of mAb 14C5.

Flow cytometric analysis was done using a FACScan flow cytometer (Becton Dickinson). Tumor cell populations were gated based on forward and side scatter variables. Data analysis was done using WinMDI (Joseph Trotter).

Radioiodination and quality control. mAb 14C5 and anti–integrin β_1 IgG1 were labeled with ^{123}I, ^{125}I, or ^{131}I. Isotopes were obtained from Bristol-Myers Squibb (Brussels, Belgium). Radioiodination was done using the Iodo-Gen method (22). Coating of the Iodo-Gen iodination reagent was done according to the manufacturer's instructions (Perbio, Erembodegem, Belgium).

For radioiodination, a mixture of iodide and mAb 14C5 dissolved in 0.1 mol/L potassium phosphate buffer (pH 8.5) was added to an Iodo-Gen-coated reaction vial for 10 minutes at room temperature. Protein-bound iodide was separated from free iodide by passing over a PD-10 column (Amersham Biosciences Europe) equilibrated with PBS-1% BSA. Quality control of radiolabeled antibody was done by size-exclusion high-performance liquid chromatography using an Ultrahydrogel 120 6-μm column (7.8 × 300 mm GPC; Waters, Brussels, Belgium) and 0.01 mol/L potassium phosphate buffer (pH 7.4) eluant at a flow rate of 0.8 mL/min.

Saturation binding study. Saturation binding studies were done with ^{125}I-labeled mAb 14C5 using LoVo and A549 cells. Twelve test

solutions (in duplicate) containing increasing amounts of radiolabeled mAb 14C5 and 0.5×10^6 cells in a total volume of 3 mL cell medium were incubated at 4°C for 2.5 hours. Then, supernatant was removed by centrifugation (8 minutes, 180 × *g*, 4°C) and cells were washed with 3 mL ice-cold PBS. For each sample, nonspecific binding was determined in the presence of 167 nmol/L of the unlabeled mAb 14C5. Radioactivity was counted by a gamma counter (Cobra II, Perkin-Elmer, Jügesheim, Germany). K_d values were determined with GraphPad Prism 3.1 software (San Diego, CA).

Internalization studies

Internalization of ^{125}I-labeled monoclonal antibody 14C5. Confluent A549 and LoVo cells in 10-cm^2 dishes were incubated with 1 μCi ^{125}I-labeled mAb 14C5, corresponding to 0.1 to 0.2 μg mAb 14C5, in 1 mL medium at 4°C for 1 hour. Cells were washed twice with ice-cold medium. Ice-cold medium (2 mL) was added and the cells were incubated at 37°C. Triplicate samples were removed at different time points, and the medium was isolated. The ^{125}I-labeled antibodies still present on the cell surface were stripped by washing the cells twice with ice-cold low-pH culture medium (pH 2.25) for 1 minute. Cell surface bound and intracellular activities were determined by measuring the activity of the acid washes and cell-associated radioactivity after treatment with low-pH medium. The fraction of internalized antibody was calculated from the intracellular activity divided by the initially bound radioactivity. At different time points, the amount of free ^{125}I in the culture supernatant was determined by passing the supernatant over a PD-10 column. The different fractions were counted with a gamma counter (Cobra II).

Confocal laser scanning microscopy. A549 and LoVo cells were confluently grown in eight-well confocal chamber slide (Lab-Tek Chamber CVG, Nalge Nunc International, Neerijse, Belgium) and incubated with 10 μg mAb 14C5 in 200 μL medium at 4°C or 37°C for various times. Subsequently, the cells were washed with PBS and the surface-bound antibody was removed by treatment with low-pH medium (pH 2.25) to improve visibility of the intracellular fraction. Cells were fixed with 3.7% formaldehyde for 20 minutes at room temperature and incubated with 0.4% Triton X-100 in PBS for 5 minutes and finally with 50 mmol/L NH_4Cl in PBS for 5 minutes. Cells were incubated overnight in PBS-1% BSA-0.02% sodium azide until incubation with Alexa Fluor 488–labeled secondary antibody and RNase H (Promega, Leiden, the Netherlands) for 1 hour at 37°C. After washing cells once with PBS and once with 50 mmol/L Tris (pH 8), 80% glycerol in 50 mmol/L Tris (pH 8) was added. Nuclei were stained by using propidium iodide. The cells were analyzed with a Zeiss LSM-410 confocal laser scanning microscope (Carl Zeiss, Zaventem, Belgium). Control samples were obtained by omitting the acidic wash step.

In vivo studies

Animal model. Male athymic mice (*nu/nu*; 5 weeks; Charles River, Brussels, Belgium) were injected s.c. into the right flank with A549 or LoVo cells (1×10^7) in 200 μL fetal bovine serum–free medium. When tumors achieved a size of 0.5 to 1 g (i.e., 3 weeks for A549 tumors and 5 weeks for LoVo tumors), biodistribution studies were initiated. Male NMRI mice (5 weeks) were obtained from an in-house breeding program. All animal studies agree with the Belgian laws and are approved by the local ethical committee for animal experiments (ECP 02/54).

Biodistribution studies. Biodistribution studies were done with athymic mice bearing A549 (0.648 ± 0.469 g) or LoVo (0.888 ± 0.468 g) tumors or with non-tumor-bearing NMRI mice. Mice were injected in the tail vein with 5 to 10 μCi ^{131}I-labeled mAb 14C5 (2.5-5 μg). Typically, groups of three were sacrificed at 1, 3, 6, 24, 48, and 168 hours after injection of radiolabeled antibody. Tumors and organs (brain, heart, liver, spleen, kidney, lung, intestine, muscle, blood, and stomach) were immediately removed, blotted dry, and weighed. Samples were counted in a gamma counter (Cobra II). Standards prepared from the injected material were counted each time with tissues and tumors, enabling calculations to be corrected for physical decay of the isotope. Radiolabeled antibody distribution over time was expressed as the percentage of injected dose/g [%ID/g; (counts/min tissue sample / counts/min standard) × 100 / weight (g)] and as tumor-to-blood ratios.

Planar gamma camera imaging. Scintigraphic imaging was done on LoVo and A549 tumor-bearing mice on a Toshiba GCA-9300A/hg single-photon emission computed tomography camera in the planar mode equipped with a low-energy high-resolution parallel-hole collimator. At 30 minutes, 6 hours, 24 hours, and 48 hours after injection of 500 μCi ^{123}I-labeled antibody (20 μg), 10-minute images were acquired in a 1,024 × 1,024–pixel matrix (field of view, 23.5 × 12.46 cm) with a photopeak window set at 15% around 159 keV. Animals were anesthetized by i.p. injection of 75 μL (1.5 mg) of a pentobarbital solution (Nembutal, 20 mg/mL, Ceva Santé Animale, Brussels, Belgium).

Results

Antigen 14C5 expression. Twenty human cell lines were examined by immunocytochemical analysis for expression of the antigen 14C5 (Table 1). Antigen 14C5 is ubiquitously expressed in the investigated cell lines (17 of 20). Not all cells stained equally, but the positive cells had a membrane-associated staining. No obvious correlation was observed

Table 1. Results of the immunoperoxidase staining for antigen 14C5 of 20 different human cancer cell lines

Cell line	14C5 reactivity
Carcinoma breast	
SK-BR-3	Positive
MCF-7	Positive
BT-20	Positive
T-47D	Positive
MDA-MB-231	Positive
Carcinoma ovary	
OVCAR-3	Positive
Carcinoma cervix	
HeLa	Positive
Carcinoma lung	
A549	Positive
Carcinoma colon	
HT-29	Positive
LoVo	Positive
Carcinoma squamous cell	
Colo16	Negative
Carcinoma pancreas	
Capan-1	Positive
Capan-2	Positive
AsPC-1	Positive
Fibrosarcoma	
HT-1080	Positive
Osteosarcoma	
791T	Positive
Glioblastoma	
LN-229	Negative
Leukemia	
MOLT-4	Negative
Melanoma	
C32	Positive
A2058	Positive

between the level of immunostaining and the tissue origin of the neoplastic cells.

Fifteen cell lines were investigated by flow cytometric analysis (Fig. 1). Significant binding was observed with C32, OVCAR-3, A2058, LoVo, and HeLa cells. The highest reactivity was found with SK-BR-3, HT-1080, A549, BT-20, HT-29, Capan-1, and Capan-2 cells.

As isotype control, an irrelevant mAb 9E10 was used. This antibody binds an intracellular epitope (c-myc) and therefore cannot bind to the cell membrane unless the antigen 14C5 is a Fc receptor or the mAb 9E10 is bound to the membrane by other Fc receptors. All plots of mAb 9E10 binding matched the autofluorescence plots of unbound cells in the presence of secondary antibody (data not shown).

Radioiodination and quality control. The radioiodination yield for mAb 14C5 and anti–integrin β_1 mAb was typically 70% to 80%. The amounts of free iodide (^{125}I, ^{123}I, or ^{131}I) in the purified iodinated mAb 14C5 were <2% and <5% for anti–integrin β_1 even after 24 hours at room temperature.

The dissociation constant (K_d) of the radiolabeled mAb 14C5 was determined for A549 and LoVo cell lines by a saturation binding assay. Figure 2 shows the saturation plot of ^{125}I-labeled mAb 14C5 to A549 and LoVo cells. Under saturated conditions, A549 cells showed higher expression of antigen 14C5 than LoVo, which agrees with the results of the flow cytometric analysis. Figure 3 shows the nonspecific binding of ^{125}I-labeled mAb 14C5 to A549 and LoVo. Nonspecific binding was determined in the presence of 167 nmol/L unlabeled mAb 14C5. mAb 14C5 bound to A549 and LoVo cells with similar affinity (K_d 0.187 ± 0.07 and 0.197 ± 0.05 nmol/L). The saturation binding curves generated were characteristics of high-affinity binding of an antibody to its antigen and merits further evaluation of the radiolabeled mAb 14C5 in a tumor model.

Internalization and dehalogenation. The degree of internalization was investigated in a RIA with A549 or LoVo cells. Both cell types were loaded with ^{125}I-labeled mAb 14C5 at 4°C for 1 hour. After removing unbound mAb 14C5, the cells were incubated at 37°C for various times to allow internalization.

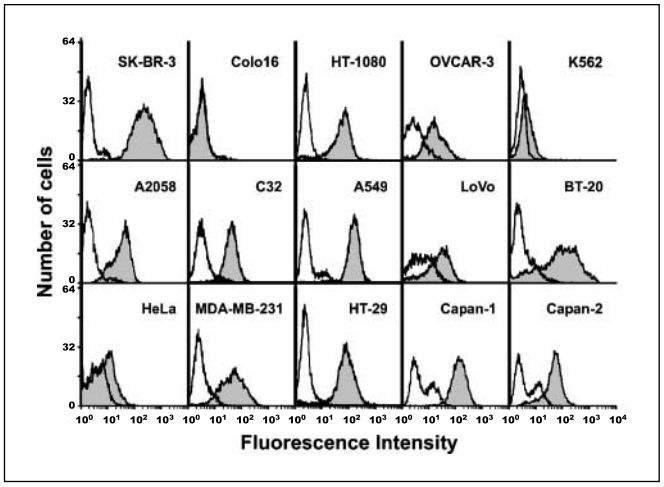

Fig. 1. Histogram of fluorescence-activated cell sorting analysis showing the binding of mAb 14C5 with various neoplastic cell lines. Cells were stained with mAb 14C5 (*filled histograms*) or anti-c-myc IgG1 (*open histograms*) isotope control mAb. Bound mAbs were detected with Alexa Fluor 488–conjugated anti-mouse IgG.

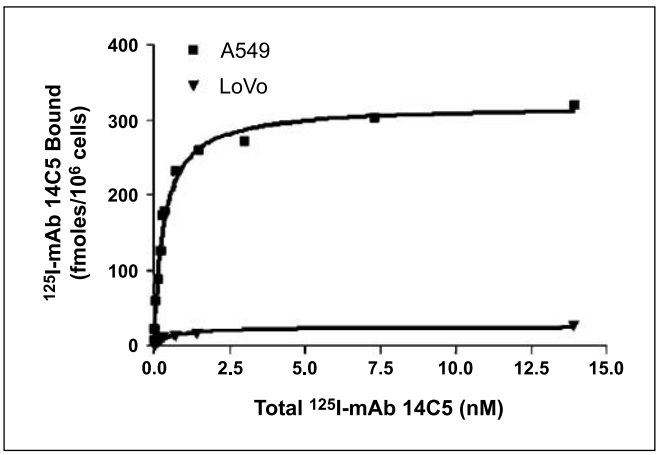

Fig. 2. Saturation binding of ^{125}I-labeled mAb 14C5 to A549 or LoVo cells. Increasing concentrations of ^{125}I-labeled mAb 14C5 were incubated with 0.5×10^6 cells at 4°C for 2.5 hours. Bound activity was isolated by centrifuging the cells and washing them twice with ice-cold PBS buffer.

The fraction of ^{125}I-labeled mAb 14C5 that remained associated with the cells after treatment with a low-pH buffer increased with longer incubation periods at 37°C from 14% (t = 0 minute) to 33% (t = 120 minutes) for LoVo cells and from 12% (t = 0 minute) to 33% (t = 120 minutes) for A549 cells (Fig. 4A).

As a control, this procedure was repeated at 4°C. Because internalization is an energy-dependent process that takes place at 37°C, at 4°C the internalization process will be inhibited. Figure 4A shows that after placing the cells at 4°C no increased radioactivity associated with both cell types could be detected. Therefore, the 10% fraction internalized ^{125}I-labeled mAb 14C5 at the start of the internalization assay (t = 0 hour, 37°C) can be considered as the acid-resistant fraction.

^{125}I-labeled mAb 14C5 showed a poor cellular retention of radioactivity with both LoVo and A549 cells (Fig. 4B). Placed at 37°C for 2 hours, A549 released 43% of radioactivity and LoVo cells released 53% of their radioactivity. At 4°C, this could be reduced to 6.6% for A549 and 11% for LoVo. Although no internalization could be detected at 4°C, the loss of radioactivity is probably due to dissociation of intact antibody. To determine whether the higher release of radioactivity during internalization could be due to catabolism of ^{125}I-labeled mAb 14C5 and subsequently the release of free iodide, the supernatants were passed over a PD-10 column at different time points. After 2 hours of incubation at 37°C, no appreciable amounts of free ^{125}I were present (<2%). This indicates that the release of radioactivity happens through intact ^{125}I-labeled mAb or ^{125}I-labeled metabolites.

In a second experiment, internalization of mAb 14C5 was monitored by confocal laser scanning microscopy. A549 cells incubated on ice showed no internalized antibody (Fig. 5A). A549 cells incubated with mAb 14C5 at 37°C showed both membrane and intracellular fluorescence (Fig. 5C), whereas cells treated with an acid wash after incubation at 37°C with mAb 14C5 showed only intracellular fluorescence (Fig. 5E). The intracellular fluorescence detected in Fig. 5C and E indicates the presence of internalized mAb 14C5. To improve visibility, the nuclei of the cells are included in Fig. 5B, D, and F. The same results were obtained with LoVo cells (data not shown).

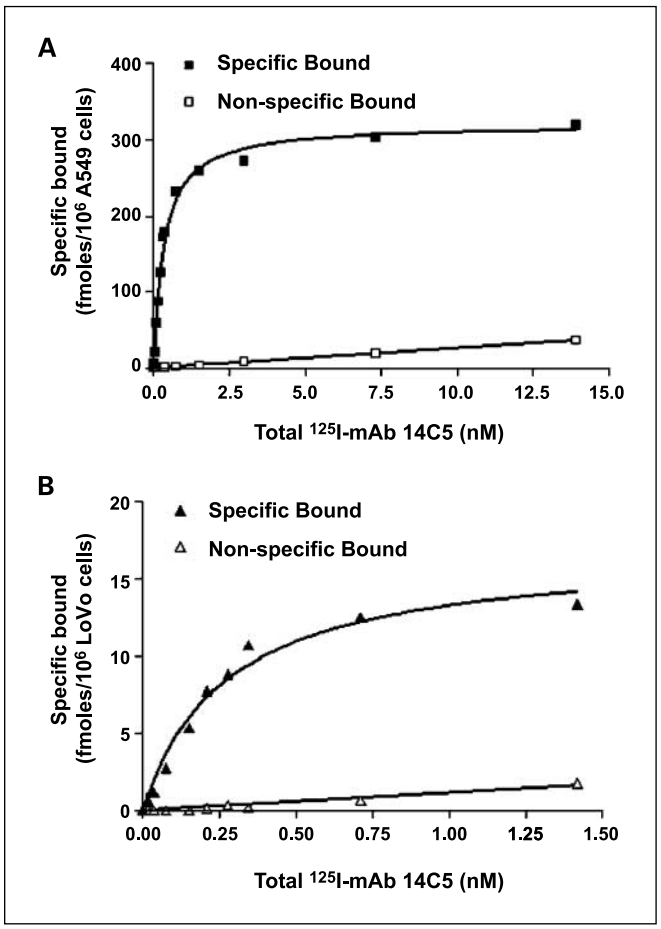

Fig. 3. Saturation binding of ^{125}I-labeled mAb 14C5 to A549 cells (*A*) and LoVo cells (*B*). Increasing concentrations of ^{125}I-labeled mAb 14C5 were incubated with 0.5×10^6 cells at 4°C for 2.5 hours. Nonspecific binding was determined in the presence of 167 nmol/L unlabeled mAb 14C5. Bound activity was isolated by centrifuging the cells and washing them twice with ice-cold PBS buffer.

Biodistribution. In a first series of experiments, pharmacokinetic properties of ^{131}I-labeled mAb 14C5 were studied in mice bearing a LoVo tumor versus untreated NMRI mice. All tissues of LoVo-bearing mice, except for the stomach, showed significantly lower accumulation of ^{131}I-labeled mAb 14C5 than tissues of NMRI mice. After 24 hours, 9%ID/g accumulated in the LoVo tumors. This tumor uptake is reflected in a decrease in radioactivity in the blood pool and other organs in the tumor-bearing mice (LoVo) compared with the non-tumor-bearing NMRI mice (control; Fig. 6). The low accumulation of radioactivity in the stomach indicates a low dehalogenation of the tracer.

LoVo cells with a low antigen 14C5 expression were compared with A549 with a high expression in a tumor model for the *in vivo* evaluation of ^{131}I-labeled mAb 14C5. The biodistribution of ^{131}I-labeled mAb 14C5 in the normal organs exhibited no significant differences between mice bearing either A549 or LoVo tumors (Fig. 7). The highest tumor uptake was observed within A549 tumors at 24 hours after injection (10.4 ± 0.8%ID/g, $n = 5$) but was not significantly higher than LoVo tumors (9.3 ± 0.8%ID/g, $n = 5$) at 24 hours after injection (Fig. 8).

Radioactive counts varied greatly with tumor size, whereas tumor-to-blood ratios showed less variation with tumor size. To investigate the factors influencing the antibody pharmacokinetics of ^{131}I-labeled mAb 14C5, the tumor uptake of mAb 14C5 versus an irrelevant anti–integrin β_1 antibody in relation to the tumor mass was studied. To reduce the number of animals needed, we focused this experiment on mice bearing A549 lung tumors. The biodistribution results of 13 mice with tumor masses varying from 0.027 to 1.9 g are shown in Fig. 9A. As a control, tumor uptake of the irrelevant IgG1 anti–integrin β_1 was measured in five mice bearing tumors varying from 0.053 to 1.2 g. Figure 9A shows a high dependency of tumor uptake on tumor mass (the smaller the tumor, the higher the uptake), whereas no such relation was seen with the nonspecific control IgG1.

In a second experiment, the antibody accretion in the tumor (%ID/g at 24 hours after injection) in relation to the cold mAb 14C5 protein dose was investigated. Mice were injected with 1 μg radiolabeled mAb 14C5 supplemented with an increasing

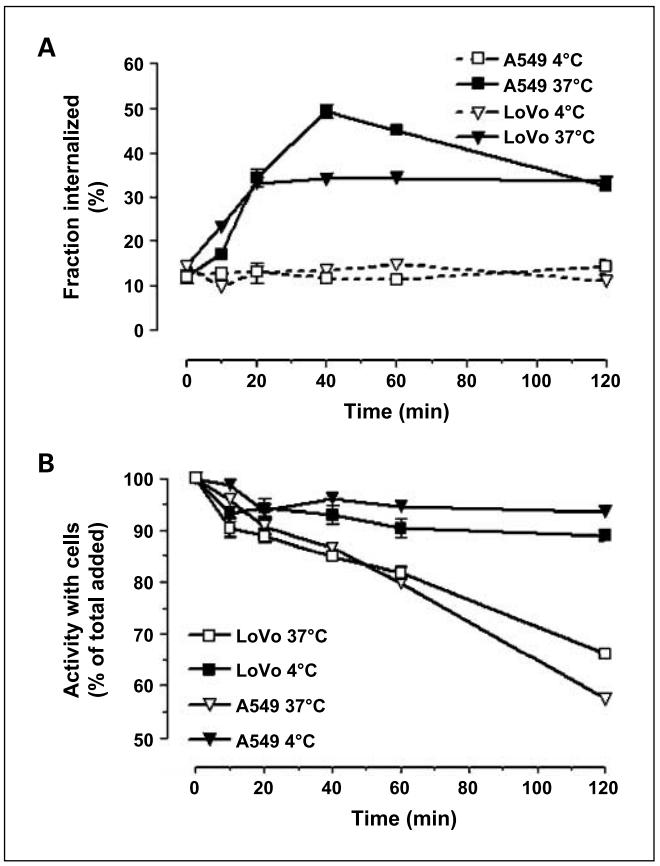

Fig. 4. Internalization and cell retention of ^{125}I-labeled mAb 14C5 by A549 and LoVo cells. *A,* internalization of ^{125}I-labeled mAb 14C5 by A549 cells (*squares*) and LoVo cells (*triangles*). Petri dishes (10 cm^2) with confluent cells were incubated with 1 μCi ^{125}I-labeled mAb at 4°C for 1 hour. Supernatant containing unbound ^{125}I-mAb 14C5 was removed. Fresh medium was added and samples were incubated at 37°C to allow internalization or at 4°C to inhibit internalization. At various time points, the ^{125}I-labeled antibodies still present on the cell surface were stripped by washing the cells with ice-cold low-pH buffer (pH 2.25) for 1 minute. The remaining radioactivity was counted as a fraction of the initially bound radioactivity. Filled symbols, experiments done at 37°C; open symbols, experiments done at 4°C. *B,* cell retention of ^{125}I-labeled mAb 14C5 by A549 cells (*squares*) and LoVo (*triangles*) cells. Petri dishes (10 cm^2) with confluent cells were incubated with 1 μCi ^{125}I-labeled mAb at 4°C for 1 hour. Supernatant containing unbound ^{125}I-mAb 14C5 was removed. Fresh medium was added and samples were incubated at 37°C to allow internalization or at 4°C to inhibit internalization. At various time points, supernatants were removed and samples were washed twice with 1 mL fresh medium. Cell-associated activity radioactivity was determined. Bars, SD.

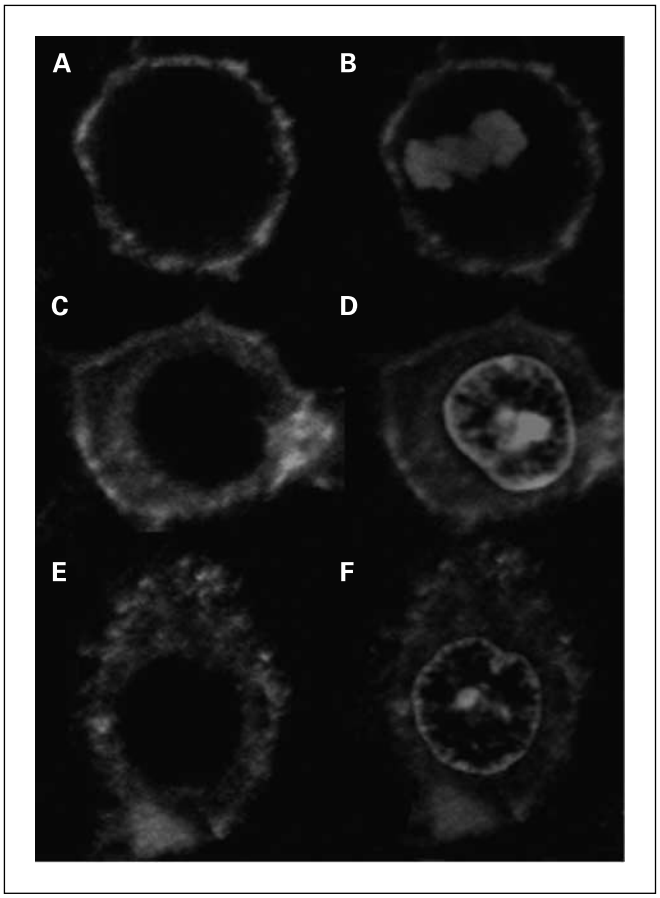

Fig. 5. Confocal laser scanning immunofluorescence images of A549 cells incubated with mAb 14C5 and Alexa Fluor 488–conjugated anti-mouse IgG. The cells shown in (*A* and *B*) were incubated with mAb 14C5 on ice for 1 hour. After incubation with Alexa Fluor 488–conjugated anti-mouse IgG, no intracellular fluorescence was detected, indicating no internalization of mAb 14C5 at 0°C. The cells shown in (*C* and *D*) and (*E* and *F*) were incubated with mAb 14C5 at 37°C for 1 hour. After incubation with Alexa Fluor 488–conjugated anti-mouse IgG, intracellular fluorescence was detected, indicating internalization of mAb 14C5 at 37°C. To improve the visibility of the intracellular fluorescence, an acid wash was used to remove the membrane-bound mAb 14C5 of cells (*E* and *F*). In addition, to improve the visibility, the nucleus is shown by staining with propidium iodide (*B*, *D*, and *F*).

amount of unlabeled mAb 14C5. Figure 9B shows that when 300 μg unlabeled mAb 14C5 is added, the uptake of ^{131}I-labeled 14C5 at 24 hours after injection is decreased from 10% to 5%ID/g. This indicates the specific uptake of mAb 14C5.

Imaging. The planar gamma camera images of tumor-bearing mice at different time intervals after injection of ^{131}I-labeled mAb 14C5 are shown in Fig. 10A-D (1, 6, 24, and 48 hours, respectively). Tumors were visible within 6 hours after tracer injection in both LoVo and A549 tumor models (Fig. 10B). The tumor-to-background contrast improved at later time points (Fig. 10C and D). As background value, a region of interest was drawn round the contralateral flank. Highest tumor-to-flank ratios were obtained at 48 hours after injection (A549 5.2 ± 1.8 and LoVo 2.0 ± 0.3: $n = 3$) for tumors weighing 1.3 ± 0.2 g. The planar imaging results varied greatly with tumor size as seen in the biodistribution data. Figure 11 shows the influence of tumor size on the visibility of A549 tumors at 48 hours after injection. A549 tumors in the right flank of nude mice, as small as 0.140 g (6 × 7 mm), could be clearly visualized.

Discussion

Prior work has shown that the mAb recognizes a cell surface antigen on mammary tumors. No antigen 14C5 could be detected in normal tissues as well as in the stroma surrounding *in situ* carcinomas of the breast. Sometimes, low-level staining of myoepithelial cells was observed in biopsies of breast tissue and in tubular cells of the kidney (14, 15).

The present data show that the expression of antigen 14C5 is not restricted to the breast cancer cell lines but is also present in varying degrees on other neoplastic human cell lines from different origins: carcinomas of ovary, cervix, lung, colon, and pancreas, sarcomas, and melanomas. Flow cytometric results showed that 9 of 15 of the investigated cell lines showed a high expression of antigen 14C5. Moreover, the A549 lung cancer cells showed the highest antigen 14C5 expression, providing a possible new target for non–small cell lung cancer (NSCLC) therapy. Although breast cancer is currently second as the leading cancer causing death in women in the United States, lung cancer is the leading cause of cancer-related mortality in both men and women, with NSCLC accounting for ~80% of all lung cancers (9, 23, 24). Today, the therapy of NSCLC has reached a plateau in improving patient survival (24). Further investigation on NSCLC-related antigen 14C5 expression is necessary and may result in antigen 14C5 as a new target for NSCLC therapy.

The antigen recognized by the mAb 14C5 has not yet been identified. No identical expression of an antigen with the same anti-cell substrate adhesion function has been found in present literature. Coene et al. (15) showed the presence of a 90-kDa protein in the SK-BR-3 lysate, suggesting that antigen 14C5 could be similar to the 85-kDa β-chain of the $\alpha_v\beta_3$ vitronectin receptor. However, when the expression of the antigen 14C5 is compared with the expression of the different integrin subunits, none of these subunits seem to overlap with the expression of the antigen 14C5 (18–20). At present, studies on the identification could not confirm the results published by Coene et al. (15). Further investigation on the identity of antigen 14C5 is being conducted.

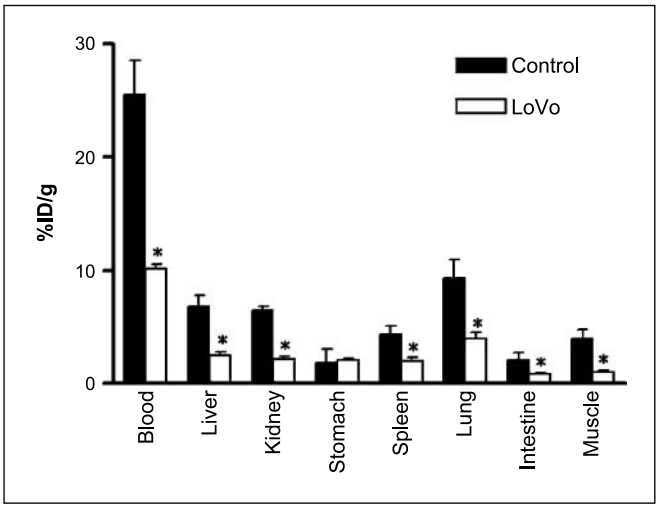

Fig. 6. Biodistribution of 5 to 10 μCi ^{131}I-labeled mAb 14C5 (2.5-5 μg) at 24 hours after injection in NMRI mice without tumor (control; *filled columns*) and nude mice bearing a LoVo colon tumor (LoVo; *open columns*). Columns, mean %ID/g ($n = 3$); bars, SD. *, $P < 0.05$, significant differences between control and mice bearing a tumor.

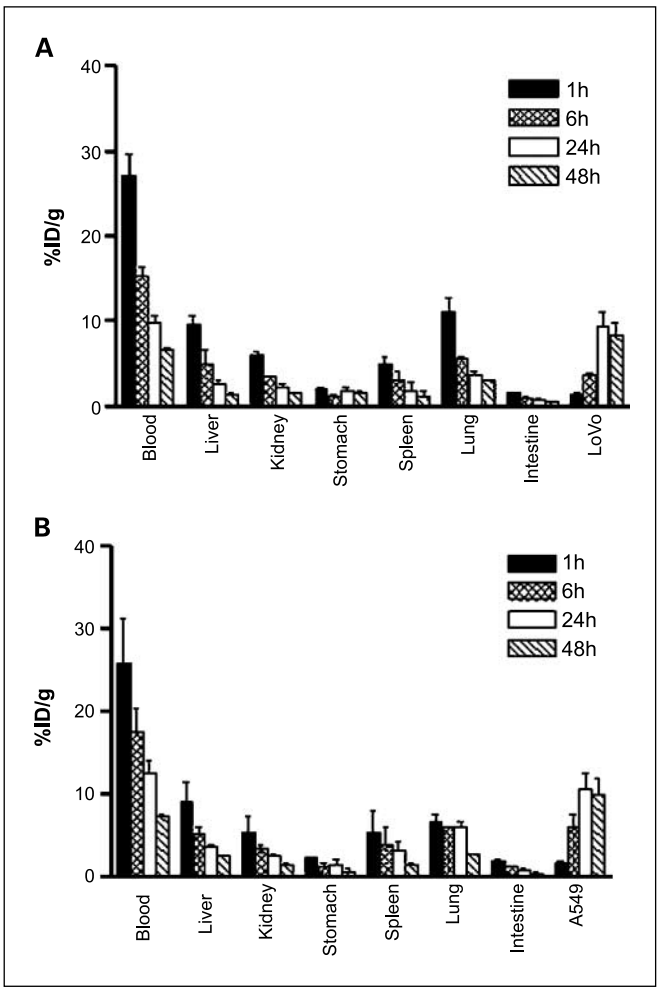

Fig. 7. Biodistribution of 5 to 10 μCi ^{131}I-labeled mAb 14C5 (2.5-5 μg) in nude mice bearing A549 (*A*) or LoVo (*B*) tumors at 1, 6, 24, and 48 hours after injection. Columns, mean %ID/g normal tissues and tumors; bars, SD ($n = 3$).

The aim of this study was to investigate the targeting properties of mAb 14C5 bound to ^{123}I and ^{131}I in nude mice bearing an A549 lung or a LoVo colon tumor. In radioimmunodetection and radioimmunotherapy, high-affinity binding with a long residence time on the specific target antigen is considered to be one of the most important properties of antibodies for achieving efficient tumor targeting. Although mAb 14C5 has not yet been evaluated in a clinical phase, the results in this article concerning the targeting properties of the ^{123}I- and ^{131}I-labeled antibody 14C5 are promising. The high affinity of mAb 14C5 for LoVo (K_d 0.20 ± 0.05 nmol/L) and A549 (K_d 0.19 ± 0.07 nmol/L) and the ubiquitous expression of the antigen 14C5 in human cancer cell lines provide a potentially useful antibody for radioimmunodetection and radioimmunotherapy. Lahorte et al. (21) reported lower affinity of mAb 14C5 for SK-BR-3 cells (K_d 0.85 ± 0.17 nmol/L) and HeLa cells (K_d 1.71 ± 0.17 nmol/L). However, binding studies were done at 37°C. In this study, we clearly showed the internalization of ^{125}I-labeled mAb 14C5 and poor cell retention at 37°C, which makes it more interesting to determine the K_d values at 4°C because at 37°C some part of radiolabeled antibody will internalize and therefore be excluded from the saturation binding leading to lower K_d values.

Internalization was shown in an *in vitro* RIA and by confocal laser scanning microscopy. Internalization can benefit therapeutic applications if there is a long-lasting association between the radionuclide and the tumor cells. Within 2 hours, ~30% of the initially membrane-bound ^{125}I-labeled mAb 14C5 was internalized in A549 and LoVo cells. Although the internalization rate of the antigen-mAb 14C5 complex is relatively slow compared with other mAbs (25–27), the dehalogenation is even slower, leading to a significant accumulation of radioactivity in the tumor cell. However, ^{125}I-labeled mAb 14C5 shows rather poor cellular retentions. Therefore, choosing another radionuclide can improve cellular retention and thus augment tumor uptake. Smith-Jones et al. (27) showed that metal chelate-labeled antibody is metabolized to leave a chelate-amino acid fragment that is typically not released from the cell and is trapped for further degradation. On the contrary, directly iodinated antibodies are metabolized within the cell, and the main metabolites of iodide and iodotyrosine are freely

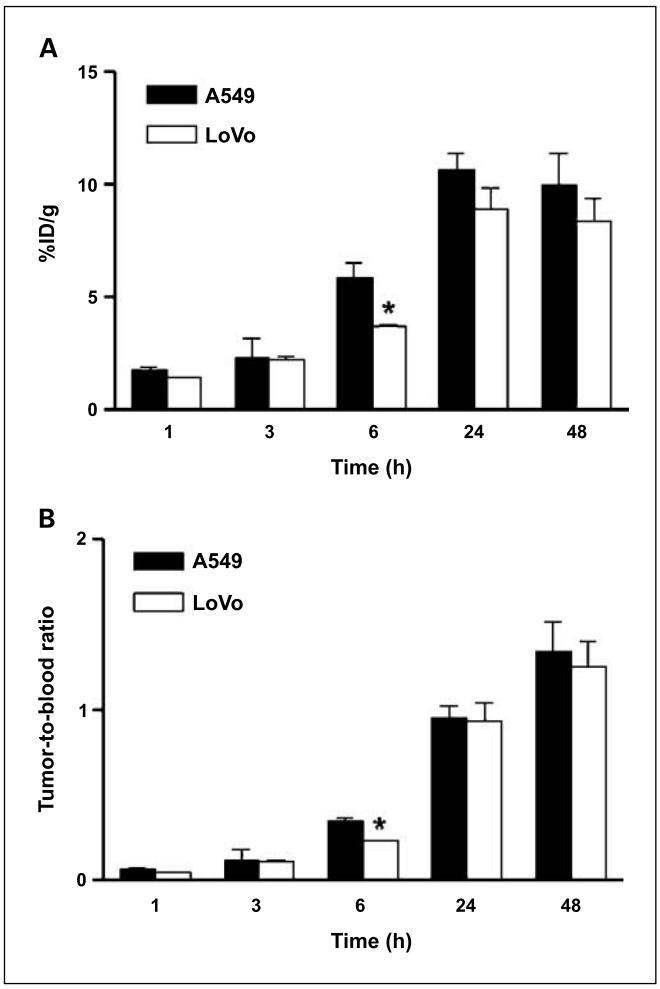

Fig. 8. Tumor uptake (*A*) and tumor-to-blood ratios (*B*) of 5 to 10 μCi ^{131}I-labeled mAb 14C5 (2.5-5 μg) in nude mice bearing an A549 lung tumor or a LoVo colon tumor at 1, 3, 6, 24, and 48 hours after injection. Columns, mean %ID/g normal tissues and tumors; bars, SD ($n = 3$). *, $P < 0.05$, significant differences between A549 and LoVo tumors.

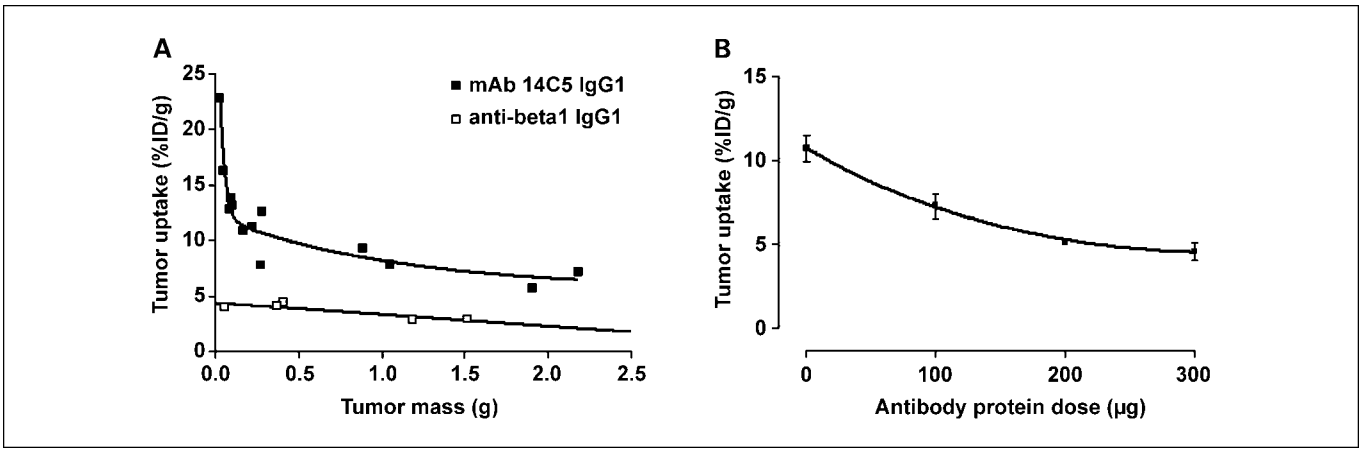

Fig. 9. Factors influencing antibody pharmacokinetics of mAb 14C5 in A549 tumor-bearing mice. *A,* tumor uptake of tumor-specific antibody, 5 to 10 μCi ^{131}I-labeled mAb 14C5 (2.5-5 μg), versus an irrelevant ^{131}I-labeled anti – integrin β_1 antibody (5 μCi, 2.5 μg) in relation to tumor mass at 24 hours after injection. *B,* antibody accretion in the A549 tumor (%ID/g at 24 hours after injection) in relation to protein dose. All mice were injected with 5 μCi radiolabeled mAb 14C5 (1 μg) supplemented with an increasing amount of unlabeled mAb 14C5 to yield the protein amounts indicated.

released from the cell. This effect can produce vastly different residence times for two differently labeled forms of the same antibody.

The high antigen 14C5 – expressing A549 lung tumors and even the low antigen 14C5 – expressing LoVo colon tumors showed good tumor uptake with ~10%ID/g tumor tissue at 24 hours after injection. This finding agrees with other high-affinity antibodies that bind effectively both high- and low-density antigen, whereas a low-affinity antibody only binds appreciably to high-density antigen because of its requirement for divalent attachment (28). This uptake is high enough to merit further evaluation in therapeutic trials (8, 13, 27, 29, 30). Via planar gamma camera imaging, A549 lung tumors as well as the LoVo colon tumors could be clearly visualized when tumors weighed ~1 g. Moreover, even when A549 lung tumors were as small as 0.14 g, they were still clearly visible by planar gamma camera imaging.

These results are encouraging, although modifications to mAb 14C5 are still possible to improve the targeting properties in patients. Many articles report on modifications that retain specificity but alter pharmacokinetics, involving the development of fragments of antibodies [e.g., F(ab')$_2$, F(ab), and scFv; refs. 31 – 33] or recombinant multivalent antibodies (34 – 39). In addition, the development of humanized antibodies should reduce the antigenicity of murine mAb 14C5 (32, 39). Furthermore, the choice of radionuclide can benefit radioimmunodetection and radioimmunotherapy. Development of radiolabeled mAb 14C5 with ^{99m}Tc or ^{111}In compared with ^{123}I for radioimmunodetection and ^{90}Y, ^{177}Lu, or ^{186}Re compared with ^{131}I for radioimmunotherapy could result in higher tumor uptake and therefore better tumor-targeting properties of radiolabeled mAb 14C5 (33, 40).

In conclusion, this study suggests that the antigen 14C5 could be an interesting new target for radioimmunodetection and radioimmunotherapy. Furthermore, because antigen 14C5 is highly expressed on a variety of tumor cells, it offers great potential for other cancer therapies besides breast cancer, including NSCLC. The fact that the antibody 14C5 can block

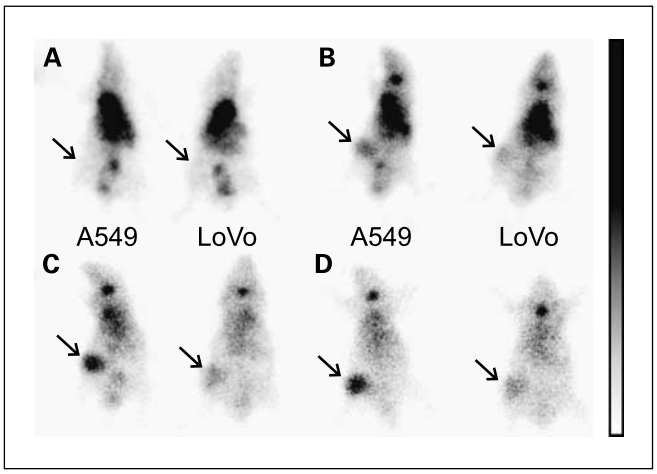

Fig. 10. Whole-body planar gamma images of 500 μCi ^{123}I-labeled mAb 14C5 (20 μg) in mice bearing a LoVo or an A549 tumor (*arrows*). Images were taken at 30 minutes (*A*), 6 hours (*B*), 24 hours (*C*), and 48 hours (*D*) after injection of radiolabeled mAb 14C5.

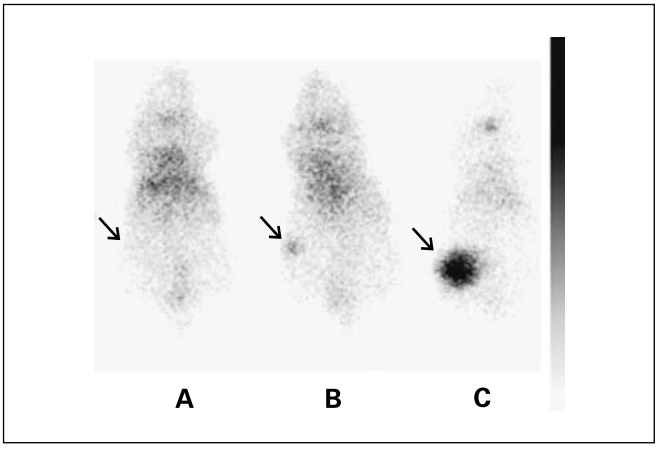

Fig. 11. Influence of tumor mass on the visibility of A549 tumors with planar gamma imaging. Whole-body planar gamma images were taken of three mice bearing an A549 tumor (*arrows*) with different size (*A,* 7 mg; *B,* 140 mg; *C,* 1 g) at 24 hours after injection of 500 μCi ^{123}I-labeled mAb 14C5 (20 μg).

cell substrate adhesion combined with the ability of mAb 14C5 to deliver a radiotoxic dose to the tumor could provide new treatment possibilities: unlabeled mAb 14C5 could prevent the settlement of undetectable metastatic cells and radiolabeled mAb 14C5 could cause tumor regression of undetectable secondary tumors. Therefore, further studies to exploit the therapeutic potential of the labeled as well as the unlabeled mAb 14C5 are warranted.

References

1. Grillo-Lopez AJ. Rituximab (Rituxan/MabThera): the first decade (1993-2003). Expert Rev Anticancer Ther 2003;3:767–79.
2. Grillo-Lopez AJ. Zevalin: the first radioimmunotherapy approved for the treatment of lymphoma. Expert Rev Anticancer Ther 2002;2:485–93.
3. Witzig TE. Zevalin (TM). Treatment of non-Hodgkin's lymphoma. Drugs Future 2002;27:563–8.
4. Kaminski MS, Estes J, Zasadny KR, et al. Radioimmunotherapy with iodide (131) I tositumomab for relapsed or refractory B-cell non-Hodgkin lymphoma: updated results and long-term follow-up of the University of Michigan experience. Blood 2000;96:1259–66.
5. Cheson BD. Radioimmunotherapy of non-Hodgkin lymphomas. Blood 2003;101:391–8.
6. Blumenthal RD, Sharkey RM, Haywood L, et al. Targeted therapy of athymic mice bearing GW-39 human colonic cancer micrometastases with ^{131}I-labeled monoclonal antibodies. Cancer Res 1992;52:6036–44.
7. Behr TM, Sharkey RM, Juweid ME, et al. Variables influencing tumor dosimetry in radioimmunotherapy of CEA-expressing cancers with anti-CEA and antimucin monoclonal antibodies. J Nucl Med 1997;38:409–18.
8. Behr TM, Blumenthal RD, Memtsoudis S, et al. Cure of metastatic human colonic cancer in mice with radiolabeled monoclonal antibody fragments. Clin Cancer Res 2000;6:4900–7.
9. Gambhir SS, Czernin J, Schwimmer J, Silverman DH, Coleman RE, Phelps MEJ. A tabulated summary of the FDG PET literature. J Nucl Med 2001;42:1–93S.
10. Nielsen UB, Adams GP, Weiner LM, James DM. Targeting of bivalent anti-erbB2 antibody fragments to tumor cells is independent of the intrinsic antibody affinity. Cancer Res 2000;60:6434–40.
11. Kobayashi H, Shirakawa K, Kawamoto S, et al. Rapid accumulation and internalization of radiolabeled herceptin in an inflammatory breast cancer xenograft with vasculogenic mimicry predicted by the contrast-enhanced dynamic MRI with the macromolecular contrast agent G6-(1B4M-Gd)(256). Cancer Res 2002;62:860–6.
12. Goldenberg DM, Nabi HA. Breast cancer imaging with radiolabeled antibodies. Semin Nucl Med 1999;29:41–8.
13. Clarke K, Lee FT, Brechbiel MW, Smyth FE, Old LJ, Scott AM. *In vivo* biodistribution of a humanized anti-Lewis Y monoclonal antibody (hu3S193) in MCF-7 xenografted BALB/c nude mice. Cancer Res 2000;60:4804–11.
14. De Potter CR, Schelfhout AM, De Smet FH, et al. A monoclonal antibody directed against a human cell membrane antigen prevents cell substrate adhesion and tumor invasion. Am J Pathol 1994;144:95–103.
15. Coene E, Schelfhout AM, De Ridder L, De Potter CR. Generation of a monoclonal antibody directed against a human cell substrate adhesion molecule and the expression of the antigen in human tissues. Hybridoma 1997;16:77–83.
16. Ruoslahti E, Pierschbacher MD. New perspectives in cell adhesion: RGD and integrins. Science 1987;238:491–7.
17. Davies J, Warwick J, Totty N, Philp R, Helfrich M, Horton M. The osteoclast functional antigen, implicated in the regulation of bone resorption, is biochemically related to the vitronectin receptor. J Cell Biol 1989;109:1817–26.
18. Koukoulis GK, Virtanen I, Korhonen M, Laitinen L, Quaranta V, Gould VE. Immunohistochemical localization of integrins in the normal, hyperplastic, and neoplastic breast. Correlations with their functions as receptors and cell adhesion molecules. Am J Pathol 1991;139:787–99.
19. Pignatelli M, Cardillo MR, Hanby A, Stamp GW. Integrins and their accessory adhesion molecules in mammary carcinomas: loss of polarization in poorly differentiated tumors. Hum Pathol 1992;23:1159–66.
20. Mizejewski GJ. Role of integrins in cancer: survey of expression patterns. Proc Soc Exp Biol Med 1999;222:124–38.
21. Lahorte CM, Bacher K, Burvenich I, et al. Radiolabeling, biodistribution, and dosimetry of (123)I-mAb 14C5: a new mAb for radioimmunodetection of tumor growth and metastasis *in vivo*. J Nucl Med 2004;45:1065–73.
22. Fraker PJ, Speck JC, Jr. Protein and cell membrane iodinations with a sparingly soluble chloroamide,1,3,4,6-tetrachloro-3a,6a-diphrenylglycoluril. Biochem Biophys Res Commun 1978;80:849–57.
23. Gridelli C. Targeted therapies in the treatment of non small cell lung cancer: reality and hopes. Curr Opin Oncol 2004;16:126–9.
24. Maione P, Rossi A, Airoma G, Ferrara C, Castaldo V, Gridelli C. The role of targeted therapy in non-small cell lung cancer. Crit Rev Oncol Hematol 2004;51:29–44.
25. Matzku S, Brocker EB, Bruggen J, Dippold WG, Tilgen W. Modes of binding and internalization of monoclonal antibodies to human melanoma cell lines. Cancer Res 1986;46:3848–54.
26. Press OW, Farr AG, Borroz KI, Anderson SK, Martin PJ. Endocytosis and degradation of monoclonal antibodies targeting human B-cell malignancies. Cancer Res 1989;49:4906–12.
27. Smith-Jones PM, Vallabahajosula S, Goldsmith SJ, et al. *In vitro* characterization of radiolabeled monoclonal antibodies specific for the extracellular domain of prostate-specific membrane antigen. Cancer Res 2000;60:5237–43.
28. Zuckier LS, Berkowitz EZ, Sattenberg RJ, Zhao QH, Deng HF, Scharff MD. Influence of affinity and antigen density on antibody localization in a modifiable tumor targeting model. Cancer Res 2000;60:7008–13.
29. Popkov M, Sidrac-Ghali S, Lusignan Y, Lemieux S, Mandeville R. Inhibition of tumour growth and metastasis of human fibrosarcoma cells HT-1080 by monoclonal antibody BCD-F9. Eur J Cancer 2001;37:2484–92.
30. Smith-Jones PM, Vallabhajosula S, Navarro V, Bastidas D, Goldsmith SJ, Bander NH. Radiolabeled monoclonal antibodies specific to the extracellular domain of prostate-specific membrane antigen: preclinical studies in nude mice bearing LNCaP human prostate tumor. J Nucl Med 2003;44:610–7.
31. Winthrop MD, DeNardo SJ, Albrecht H, et al. Selection and characterization of anti-MUC-1 scFvs intended for targeted therapy. Clin Cancer Res 2003;9:3845–53S.
32. Goldenberg DM. Targeted therapy of cancer with radiolabeled antibodies. J Nucl Med 2002;43:693–713.
33. Adams GP, Shaller CC, Dadachova E, et al. A single treatment of yttrium-90-labeled CHX-A″-C6.5 diabody inhibits the growth of established human tumor xenografts in immunodeficient mice. Cancer Res 2004;64:6200–6.
34. Schoonjans R, Willems A, Schoonooghe S, et al. Fab chains as an efficient heterodimerization scaffold for the production of recombinant bispecific and trispecific antibody derivatives. J Immunol 2000;165:7050–7.
35. Goel A, Colcher D, Baranowska-Kortylewicz J, et al. Genetically engineered tetravalent single-chain Fv of the pancarcinoma monoclonal antibody CC49: improved biodistribution and potential for therapeutic application. Cancer Res 2000;60:6964–71.
36. Todorovska A, Roovers RC, Dolezal O, Kortt AA, Hoogenboom HR, Hudson PJ. Design and application of diabodies, triabodies and tetrabodies for cancer targeting. J Immunol Methods 2001;248:47–66.
37. Power BE, Doughty L, Shapira DR, et al. Noncovalent scFv multimers of tumor-targeting anti-Lewis(y) hu3S193 humanized antibody. Protein Sci 2003;12:734–47.
38. Olafsen T, Tan GJ, Cheung CW, et al. Characterization of engineered anti-p185HER-2 (scFv-CH3)2 antibody fragments (minibodies) for tumor targeting. Protein Eng Des Sel 2004;17:315–23.
39. Reff ME, Heard C. A review of modifications to recombinant antibodies: attempt to increase efficacy in oncology applications. Crit Rev Oncol Hematol 2001;40:25–35.
40. Koppe MJ, Bleichrodt RP, Soede AC, et al. Biodistribution and therapeutic efficacy of (125/131)I-, (186)Re-, (88/90)Y-, or (177)Lu-labeled monoclonal antibody MN-14 to carcinoembryonic antigen in mice with small peritoneal metastases of colorectal origin. J Nucl Med 2004;45:1224–32.

Clinical Cancer Research

In vitro and *In vivo* Targeting Properties of Iodine-123- or Iodine-131–Labeled Monoclonal Antibody 14C5 in a Non–Small Cell Lung Cancer and Colon Carcinoma Model

Ingrid Burvenich, Steve Schoonooghe, Bart Cornelissen, et al.

Clin Cancer Res 2005;11:7288-7296.